Pathogenic Mechanism of Mouse Brain Damage Caused by Oral Infection with Shiga Toxin-Producing *Escherichia coli* O157:H7

EIJI KITA,[1]* YOSHIHISA YUNOU,[1] TAKAAKI KURIOKA,[1] HIROKO HARADA,[1]
SHINJI YOSHIKAWA,[1] KEIICHI MIKASA,[2] AND NOBUTAKA HIGASHI[1]

*Department of Bacteriology[1] and Department of Medicine II,[2] Nara Medical University,
Kashihara, Nara 634-8521, Japan*

In a previous study, we showed that infection with Shiga toxin (Stx)-producing *Escherichia coli* O157:H7 (strain Sm^rN-9) caused neurologic symptoms in malnourished mice with positive immunoreactions of Stx2 in brain tissues. The present study explores the mechanism of how Stx injures the vascular endothelium to enter the central nervous system in mice. Oral infection with strain Sm^rN-9 elicited a tumor necrosis factor alpha (TNF-α) response in the blood as early as 2 days after infection, while Stx was first detected at 3 days post-infection. In the brain, TNF-α was detected at day 3, and its quantity was increased over the next 3 days. Frozen sections of the brains from moribund mice contained high numbers of apoptotic cells. Glycolipids recognized by an anti-Gb3 monoclonal antibody were extracted from the brain, and purified Stx2 was able to bind to the glycolipids. In human umbilical vascular endothelial cells (HUVEC) cultured with fluorescein-labeled Stx2 (100 ng/ml), TNF-α (20 U/ml) significantly facilitated the intracellular compartmentalization of fluorescence during 24 h of incubation, suggesting the enhanced intracellular processing of Stx2. Consequently, higher levels of apoptosis in HUVEC were found at 48 h. Short-term exposure of HUVEC to Stx2 abrogated their apoptotic response to subsequent incubation with TNF-α alone or TNF-α and Stx2. In contrast, primary exposure of HUVEC to TNF-α followed by exposure to Stx2 alone or TNF-α and Stx2 induced apoptosis at the same level as obtained after 48-h incubation with these two agents. These results suggest that the rapid production of circulating TNF-α after infection induces a state of competence in vascular endothelial cells to undergo apoptosis, which would be finally achieved by subsequent elevation of Stx in the blood. In this synergistic action, target cells must be first exposed to TNF-α. Such cell injury may be a prerequisite to brain damage after infection with Stx-producing *E. coli* O157:H7.

Shiga toxin (Stx)-producing enterohemorrhagic *Escherichia coli* strains of serotype O157:H7 cause hemorrhagic colitis, which is often followed by hemolytic-uremic syndrome (HUS) and/or acute encephalopathy (8, 12). Stx plays a critical role in the pathogenesis of diarrhea caused by Stx-producing *E. coli* O157:H7, which has been demonstrated by several animal studies (13, 23, 33, 35). However, the pathogenesis of these severe combined diseases is not well understood. Based on several experimental findings (2, 26), one possible mechanism for the development of such complications has been proposed: Stx produced by *E. coli* O157:H7 hematogenously disseminates from the gut to the kidney (36) or the brain (32).

Our previous study (16) showed that when mice with protein calorie malnutrition (PCM) by feeding on a low-protein diet were infected intragastrically with a clinical isolate of Stx-producing *E. coli* O157:H7, they died from brain damage but not from renal damage. In only mice developing neurologic symptoms, Stx was detectable in the blood, and immunoreactions of Stx were demonstrated in the brain tissues by immunocytochemical staining. Such findings may support the assumption that Stx hematogenously enters the brain. Since the enhanced susceptibility of mice with PCM to Stx-producing *E. coli* O157:H7 is explained by the nondevelopment of an intestinal physical barrier (16), a relatively large amount of Stx may be absorbed into the bloodstream in such animals compared to well-nourished ones. However, the mechanism where-

by Stx enters the central nervous system (CNS) from the bloodstream is not known.

Stx is known to induce apoptosis in group I Burkitt's lymphoma (20) and a subset of germinal center B cells (30) expressing Gb3/CD77 as a functional receptor for Stx. Moreover, Fujii et al. (2) have reported that Stx exhibits a direct effect on brain nerve cells and also demonstrated (3, 4) that in rabbits Stx2 may leak from the bloodstream into the cerebrospinal fluid, which leads to an increase in the paracellular permeability through the blood-brain barrier (BBB) around the third ventricle. If this is the case, Stx must first injure the vascular endothelium in order to enter the CNS. However, vascular endothelial cells, unlike Vero cells, are resistant to Stx cytotoxicity (31). Moreover, it was demonstrated that tumor necrosis factor alpha (TNF-α) could induce apoptosis in endothelial cells in the presence of inhibitors of protein synthesis (25, 39), although normally this cytokine does not injure endothelial cells (24). In addition, many investigators have shown that cooperation between Stx and inflammatory cytokines including interleukin (IL)-1β (14, 18) and TNF-α (9, 11, 18) are involved in injury of vascular endothelial cells and in eliciting the pathologic changes in HUS. Since Stx is a strong protein synthesis inhibitor for cells expressing Gb3/CD77, we speculated that Stx may potentiate TNF-α-induced apoptosis in vascular endothelial cells.

Thus, the aim of this study was to examine how inflammatory cytokines and Stx exert the synergistic effect on injury of vascular endothelial cells and also to determine whether infection with Stx-producing *E. coli* O157:H7 causes apoptosis in the mouse brain. In addition, we attempted to demonstrate the presence of Stx receptors in mouse brain tissues. Results ob-

* Corresponding author. Mailing address: Department of Bacteriology, Nara Medical University, 840, Shijyocho, Kashihara, Nara 634-8521, Japan. Phone: 81-744-29-8839. Fax: 81-744-29-7375. E-mail: eijikita@nmu-gw.cc.naramed-u.ac.jp.

tained here support the concept that hematogenously disseminated Stx causes damage to the vascular endothelium in cooperation with circulating TNF-α and leaks into the cerebrospinal fluid. In this pathogenic process, TNF-α accelerates the intracellular processing of Stx, which in turn, may potentiate TNF-α-induced apoptosis in vascular endothelial cells. Furthermore, such a synergistic effect may occur in the brain, since TNF-α production and functional receptors for Stx were found in brain extracts.

MATERIALS AND METHODS

Microorganisms. *E. coli* O157:H7 strain Sm^{r}N-9, which is resistant to streptomycin (100 µg/ml) and is able to produce Stx1 and -2, was used (16). *E. coli* NP-4 isolated from the stool of a healthy adult was used as a control strain (16). Both strains were preserved in gelatin-charcoal disks at −20°C. Before use, one of the preserved disks was dissolved in 1 ml of tryptic soy broth (Difco Laboratories, Detroit, Mich.), and 100 µl of this bacterial suspension was inoculated into 10 ml of fresh tryptic soy broth. For infection study, bacteria were harvested by centrifugation from broth culture after growth overnight at 37°C, washed, and resuspended in sterile phosphate-buffered saline (PBS; 10 mM, pH 7.2) at a concentration of 2×10^7 CFU/ml.

Mouse infection. Specific-pathogen-free, 3-week-old female C57BL/6 mice that had been weaned were purchased from Charles River (Tokyo, Japan). Animals were fed a low-protein diet (5% protein) (Oriental Bio Service Inc., Kyoto, Japan) for 2 weeks to achieve PCM as described previously (16).

Mice 5 weeks of age were infected intragastrically with 2×10^6 CFU of strain Sm^{r}N-9 in a volume of 0.1 ml through a stainless steel catheter with a blunt end (outer diameter, 0.45 mm; Natsume Seisakusyo Co., Tokyo, Japan). Mice were neither fasted nor treated with streptomycin prior to infection, and they were fed the low-protein diet even after infection.

Extraction of neutral glycolipids from mouse brains. The brain was removed from the bony skeleton after mice were sacrificed by intravenous injection of pentobarbital at 0.5 ml/kg of body weight. Brains obtained from three mice were washed in saline and homogenized in 5 ml of chloroform-methanol (2:1, vol/vol) by vigorous vortexing and sonication. The homogenate was heated at 60°C for 1 h and centrifuged at $2,000 \times g$ for 20 min. The supernatant of chloroform-methanol was collected, and cell residue was reextracted with chloroform-methanol and centrifuged. These two extracts were combined and evaporated to dryness under a stream of nitrogen. The residue was heated at 60°C for 1 h in chloroform-methanol (2:1, 1:1, and 1:2) and centrifuged. The supernatant of chloroform-methanol (total lipid extract) was collected and dried under a stream of nitrogen. This extract was then partitioned into aqueous and organic fractions with diisopropyl ether–1-butanol–100 mM NaCl (6:5:4, vol/vol/vol) by a modification of the technique of Ladisch and Gillard (17). The fractions were dried, and the aqueous fraction was resuspended in chloroform-methanol-water (1:10:10, vol/vol/vol). To remove salts and water-soluble contaminants, reversed-phase chromatography was performed on RP$_{18}$ cartridges (Waters Associates, Milford, Mass.) (15). The desalted extract was separated into acidic and neutral fractions by chromatography on a column of DEAE-Sephadex A-25 (Pharmacia Biotechnology, Tokyo, Japan) (15, 27). Neutral fractions eluted with chloroform-methanol-water (30:60:8, vol/vol/vol) from the DEAE column were evaporated to dryness. Then dried materials were dissolved in a minimum amount of chloroform and incubated at 40°C for 30 min after addition of 6 N NH$_4$OH in methanol. After incubation, treated samples were dried, dissolved in chloroform-methanol (2:1, vol/vol), and used as the brain neutral glycolipid extract.

In situ DNA fragmentation analysis. DNA fragmentation was determined by the in situ TUNEL (terminal deoxynucleotidyltransferase (TdT)-mediated dUTP-biotin nick end labeling) technique (6), which is based on the specific binding of TdT to 3′-OH ends of DNA. For this assay, frozen sections of mouse brains obtained at 10 days postinfection and formalin-fixed monolayers of cultured human umbilical venous endothelial cells (HUVEC) were used. Frozen sections (3 µm thick) of brains or formalin-fixed HUVEC monolayers were treated with proteinase K (Boehringer Mannheim, Indianapolis, Ind.) at a concentration of 20 µg/ml for 20 min, rinsed, blocked with 1% bovine serum albumin and 0.003% Triton X-100 in 10 mM PBS for 30 min at room temperature, and then rinsed again. These treated preparations were immersed in TdT (0.5 U/µl) and 1 mM biotin-16-dUTP in reaction buffer (Boehringer Mannheim) and incubated in a humid atmosphere at 37°C for 1 h. The reaction was stopped with termination buffer (300 mM NaCl, 30 mM sodium citrate [pH 7.2]). These sections were washed with distilled water, blocked with 2% bovine serum albumin in PBS for 10 min, rinsed again with distilled water, immersed in PBS for 5 min at room temperature, and then incubated with an avidin-peroxidase complex (Boehringer Mannheim) diluted 1:600 in PBS for 30 min at 37°C. Color development was done with diaminobenzidine (DAB)-H$_2$O$_2$. The number of TUNEL-positive cells in experimental and control materials was counted under a light microscopy in a blinded fashion by three different investigators. Apoptotic cells were identified by dark-brown staining in the nucleus. On each slide, approximately 200 cells were evaluated for the presence of apoptotic cells. The background number of TdT-positive cells in controls was subtracted from the number of TUNEL-positive cells in experimental material.

TLC-blot analysis. Brain neutral glycolipids were spotted onto two Silica Gel 60 high-performance thin-layer chromatography (TLC) plates (0.2 mm thick; Merck AG, Darmstadt, Germany) and were developed in chloroform-methanol-water (65:25:4, vol/vol/vol) to 7 cm from the origin. TLC standards of neutral glycolipids (Accurate Chemical & Scientific Corporation, Westbury, Conn.) were used as reference. After chromatographic separation, the plates were dried, and one of them was sprayed with orcinol reagent (Sigma) to identify each glycolipid in brain samples and standard preparations. For immunoblotting, the other plate was coated with 0.1% polyisobutyl-methacrylate (Polyscience, Warrington, Pa.), air dried, and sprayed with 20 mM Tris-HCl–150 mM NaCl–5 mM MgCl$_2$–0.15 mM CaCl$_2$ (pH 7.4) (TNMC). The plate was covered with a polyvinylidene difluoride (PVDF) membrane (Atto Co. Ltd., Tokyo, Japan) and then glass membrane filters (GF/A, Whatman Paper Ltd., Maidstone, United Kingdom). This assembly was pressed with an electric iron at 180°C for 30 s. The blot membrane was dried, rehydrated by being placed on the surface of TNMC, and then incubated with 10% horse serum in TNMC for 1 h at 37°C to block excess binding capacity.

Immunodetection. To examine Gb3, the blot membrane was washed with TNMC after blocking and overlaid with an anti-P^k monoclonal antibody (MAb) (specificity, Galα 1-4Gal β1-4 Glcβ1-1Cer moiety of Gb3; isotype, murine immunoglobulin M [IgM]) (Accurate Chemical & Scientific Corporation) (1) diluted 1:8 in 10% horse serum in TNMC. After overnight incubation at 4°C, the membrane was washed five times with TNMC and then incubated for 1 h with a 1:100 dilution of peroxidase-conjugated goat anti-mouse IgM F(ab′)$_2$ (Organon Teknika, Durham, N.C.). The membrane was washed five times with TNMC, and the color reaction was performed with DAB-H$_2$O$_2$.

The glycolipids to which Stx2 bound were detected on the blot membrane as follows. After blocking, the blot membrane was overlaid with TNMC containing Stx2 (1 µg/ml) purified by the method of Yutsudo et al. (39) and incubated at 37°C for 30 min. After incubation, the membrane was washed five times with TNMC and overlaid with a murine MAb to Stx2 (IgG class; 1 µg/ml; Toxin Technology, Inc., Sarasota, Fla.) at 4°C overnight. Then the membrane was washed and treated for 1 h at 37°C with a 1:200 dilution of biotinylated anti-mouse IgG F(ab′)$_2$ (Organon Teknika). Thereafter, the membrane was incubated with an avidin-peroxidase complex (Boehringer Mannheim) diluted 1:600 in TNMC for 30 min at 37°C. The color reaction was performed with DAB-H$_2$O$_2$.

Cytokine assay. IL-1β, IL-6, IL-10, and TNF-α in brain homogenates and serum were quantified by enzyme-linked immunoassay (EIA) using commercially available kits (Genzyme, Cambridge, Mass.). Whole brains were removed from mice killed by exsanguination and were minced in 10 mM phosphate buffer (pH 7.2) containing 0.5 mM phenylmethylsulfonyl fluoride (Sigma) and 0.05% Triton X-100. Then they were homogenized with a sonicator (Tomy Handy Sonicator; Tomy Seiko Co. Ltd., Tokyo, Japan) at 4°C. These homogenates were centrifuged at $30,000 \times g$ for 20 min, and supernatants were collected for cytokine assay. A standard curve for each cytokine was constructed with the appropriate recombinant murine cytokine (Genzyme) incorporated into normal mouse serum or brain extract. For measurement of serum cytokines at each time point, serum was collected from three mice, and individual samples were divided into three 100-µl aliquots. Data were obtained from three different experiments. With these EIA kits, the limits of detection for IL-1β, IL-6, IL-10, and TNF-α in serum were 15, 18, 13, and 14 pg/ml, respectively. The limit of detection for cytokines in brain extracts was 30 pg/100 mg of protein, irrespective of the cytokine used for measurement. The protein content of each homogenate was determined by the dye-binding assay using a DC protein assay kit (Bio-Rad Laboratories, Hercules, Calif.).

Measurement of Stx antigen. Stx levels in the blood were determined with an EIA kit (Premier EHEC; Meridian Diagnostic, Inc., Cincinnati, Ohio) as described previously (16). Blood was obtained from the ophthalmic arteries of infected mice. Serum was separated from clotted blood by centrifugation and then concentrated 20-fold by ultrafiltration before assay. Twenty microliters of each concentrated serum sample was mixed with 4 volumes of the sample dilution buffer, and then 100 µl of each mixture was assayed with the EIA kit reagents. A standard curve was constructed with the purified Stx1 incorporated into normal mouse serum, and results were expressed as Stx1 amounts (picograms) per milliliter of neat serum (16). With this EIA kit, the limit of detection for Stx1 was 20 pg/ml of neat serum.

Labeling of Stx2 with fluorescent dye. Lyophilized Stx2 was dissolved at a concentration of 1.2 mg/ml in 200 µl of PBS and labeled with Oregon Green 488 (37), using a FluoReporter protein labeling kit (F-6153; Molecular Probes, Inc., Eugene, Oreg.). Labeling was done exactly as instructed by the manufacturer. The molar ratio of Oregon Green 488 to Stx2 was 20, and the fluorescent dye-Stx2 conjugate was recovered using a spin column provided by the manufacturer. The labeled Stx2 was dialyzed against PBS, and the final labeled preparation was confirmed to retain the same degree of verocytotoxicity as the unlabeled material.

Determination of uptake of Stx2 by HUVEC. HUVEC were purchased from Dainipon Pharmaceutical Co. (Tokyo, Japan). Basal culture medium was alpha minimal essential medium (GIBCO, Grand Island, N.Y.) with 20% heat-inactivated fetal bovine serum (HyClone Laboratories, Logan, Utah), 100 µg of heparin (Sigma) per ml, 50 U of penicillin per ml, and 50 µg of streptomycin per ml
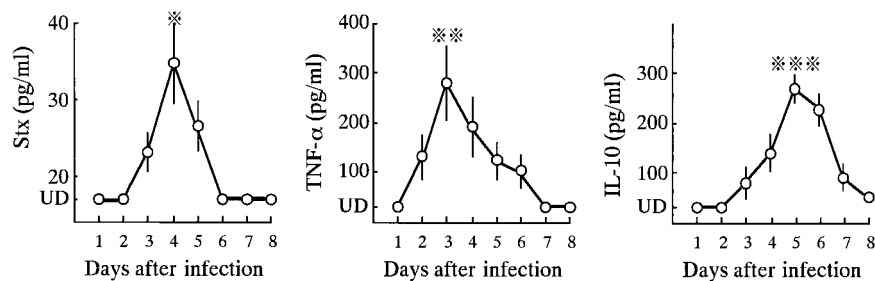
FIG. 1. Serum levels of Stx, IL-10, and TNF-α after intragastric inoculation of 2×10^6 CFU of Sm^{r}N-9 in PCM mice. Data were obtained from five different experiments, each using three mice. Each point represents the mean value of 15 determinants, and bars indicate SD. ❋, $P < 0.05$ compared to days 2 and 3; ❋❋, $P < 0.05$ compared to days 2, 5, and 6 but not significant compared to day 4; ❋❋❋, $P < 0.01$ compared to days 3 and 7, and $P < 0.05$ compared to days 4, but not significant compared to day 6; UD, undetectable levels.

(defined as complete medium [CM]). HUVEC were suspended at a concentration of 10^3/ml in CM supplemented with 10 μl of bovine retinal extract per ml (CM-BRE) prepared as described previously (7, 29). HUVEC were seeded in culture dishes (6-cm diameter; Falcon; Becton Dickinson Labware, Oxnard, Calif.) coated with human fibronectin (1 μg/cm^2) and incubated at 37°C in humidified 5% CO_2.

The cells were fed every other day with fresh CM-BRE and were detached with a mixture of 0.5% collagenase S-1 (Nitta Gelatin, Osaka, Japan) and 0.02% EDTA in Ca^{2+}- and Mg^{2+}-free balanced salt solution when the culture became subconfluent. Washed detached cells were distributed into fibronectin-coated chambers of Lab-Tek chamber slides (eight-chamber type; Nunc Inc., Naperville, Ill.) at a concentration of 5×10^4 per chamber in a volume of 400 μl of CM-BRE. After 12 h of incubation, fluorescent dye-labeled Stx2 was added to each chamber at a concentration of 100 ng/ml. This dose of the labeled toxin was equivalent to about 10^5 CD$_{50}$, where CD$_{50}$ is defined as the dose required for 50% death of Vero cells. After 12 and 24 h, cell monolayers were washed three times with PBS before microscopic observation. Fifty randomly selected HUVEC were observed under an Olympus (Tokyo, Japan) BX50 fluorescence microscope. The intensity of fluorescence per cell was quantified with a computer-assisted confocal laser microscope (InSIGHT plus-IQ; Meridian Instruments Inc., Okemos, Mich.) as described elsewhere (10, 31), and the mean intensity per cell was determined by measuring the fluorescence intensity of 50 individual cells in three different fields on a slide.

Synergistic effect of cytokines and Stx2 on cell damage to HUVEC. Purified Stx2 was added at a final concentration of 100 ng/ml to HUVEC monolayers in the presence or absence of human recombinant TNF-α, IL-1β, or IL-6 (Genzyme). Incubation was carried out at 37°C for 72 in 5% CO_2, and the number of apoptotic cells was determined by the TUNEL method. The optimal doses of these three cytokines were initially determined by their ability to stimulate HUVEC to release soluble intercellular adhesion molecule I (sICAM-1) without cell damage twice as much as unstimulated cells produce in culture supernatants: 20 U of TNF-α per ml, 15 U of IL-1β per ml, and 35 U of IL-6 per ml, respectively. A human sICAM-1 EIA kit (Endogen, Woburn, Mass.) was used to measure sICAM-1 in culture supernatants. Anti-Stx2 MAb (Toxin Technology) and anti-human TNF-α MAb (Genzyme) were used to neutralize the activity of Stx2 and TNF-α, respectively.

Cytotoxicity was determined by measuring lactate dehydrogenase (LDH) in culture supernatants with a nonradioactive cytotoxicity assay kit (Cell Titer 96 aqueous nonradioactive cell proliferation assay; Promega Corporation, Madison, Wis.). HUVEC (10^5 cells) in 100 μl of CM-BRE, devoid of phenol red, were distributed into fibronectin-coated wells of 24-well culture plates. After 2 h of incubation, Stx2 and/or cytokines were added, and cytotoxic assay was performed 72 h later. Percent cytotoxicity was expressed as {(experimental − target spontaneous-background)/(target maximum − target spontaneous-background)} $\times$ 100. Maximum LDH release from target HUVEC was determined after complete lysis of the cells with 0.8% Triton X-100.

To confirm the nucleosomal ladder pattern of DNA degradation in HUVEC, DNA was extracted from the cells cultured in 24-well culture plates at 48 h of incubation using a DNA extraction kit (Stratagene, La Jolla, Calif.). Precipitated DNA was air dried and suspended in 10 mM Tris–1 mM EDTA, pH 7.4. The DNA solution was subjected to conventional electrophoresis (2% agarose for 1.5 h at 10 V/cm). DNA was visualized with ethidium bromide.

Sequential treatment of HUVEC with Stx2 and TNF-α. HUVEC monolayers were pulsed with either Stx2 (100 ng/ml) or TNF-α (20 U/ml) and incubated at 37°C for 6 h in 5% CO_2. At the end of pulsing, monolayers were washed four times with CM-BRE. Thereafter, TNF-α (20 U/ml) was added to the monolayers pulsed with Stx2, and Stx2 (100 ng/ml) was added to those pulsed with TNF-α. After 42 h of incubation, TUNEL assay was performed. Monolayers of HUVEC incubated with Stx2 (100 ng/ml) and TNF-α (20 U/ml) for 48 h were used as a positive control, and 44.9% ± 6.4% (mean ± standard deviation [SD]) of cultured cells became TUNEL positive.

Statistics. The significance of differences observed was assessed by the Kruskal-Wallis one-way analysis of variance in comparison of percentage of

TUNEL-positive cells, cytotoxicity, and fluorescence intensity. $P < 0.05$ was considered significant.

RESULTS

Measurement of Stx and cytokines in mouse serum. Stx was elevated to detectable levels in the serum from days 3 through 5 when PCM mice were infected intragastrically with 2×10^6 CFU of strain Sm^{r}N-9 (Fig. 1); serum levels peaked at day 4 (mean, 34.8 ± 4.6 pg/ml). In contrast, Stx was not detected from days 1 through 8 in well-nourished mice inoculated with the same dose of Sm^{r}N-9.

Among cytokines, TNF-α was first elevated to detectable levels in the sera of PCM mice at day 2 (mean, 135.2 ± 40.2 pg/ml); the peak serum level was as much as 300 pg/ml. Thereafter, serum levels of TNF-α decreased gradually over 4 days. On the other hand, the IL-10 level slowly increased in the sera of infected PCM mice. In contrast, serum IL-1β levels remained lower than the limit of detection from days 1 through 8. None of these cytokines was detected in the sera of PCM mice after infection with 2×10^6 CFU of *E. coli* NP-4. In addition, neither Stx, TNF-α, IL-1β, nor IL-10 was detected in the sera of well-nourished mice inoculated with 2×10^6 CFU of Sm^{r}N-9 from days 1 through 8.

Determination of cytokine levels in the brain. Cytokine levels in the brain tissues of infected PCM mice were measured at 3 and 6 days after infection. Only TNF-α was detected (54 ± 25 pg per 100 mg of tissue protein) in the brain tissues of PCM mice at 3 days postinfection: there was no TNF-α response in the brain during the first 2 days of infection. Levels of TNF-α in the brain were increased approximately by twofold (98 ± 34 pg per 100 mg of tissue protein) at 6 days after infection. Among other cytokines, only IL-10 was measurable in the brain tissues of infected PCM mice at 6 days postinfection (45 ± 9 pg per 100 mg of tissue protein), but neither IL-1β nor IL-6 was detected on days 3 and 6 of infection. Neither PCM mice given 2×10^6 CFU of *E. coli* NP-4 nor well-nourished mice infected with the same dose of Sm^{r}N-9 showed cytokine responses in the brain.

Detection of Stx receptors in the brain. To test for the presence of Stx-binding glycolipids (Gb3) in the mouse brain, neutral glycolipid extracts of brain tissues were prepared, separated by TLC (Fig. 2, lane B), and compared to TLC of standard neutral glycolipids (lane A). Gb3 was identified by TLC-blot assay using an anti-P^k MAb recognizing the specific epitope of Gb3. Immunostaining demonstrated the presence of glycolipids recognized by an anti-P^k MAb in the brain neutral glycolipid fraction (lane D) and the standard neutral glycolipids (lane C). In addition, a TLC-blotted PVDF membrane (the same as used for lane D) was incubated with the purified Stx2, and the glycolipid-Stx complexes were identified by immuno-
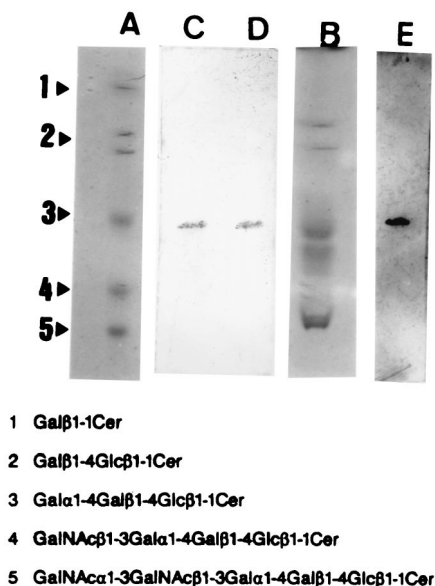
FIG. 2. Demonstration of functional receptors for Stx2 in the neutral glycolipid fraction of mouse brain. Standard mixtures of neutral glycolipids (lane A) and neutral glycolipids of the mouse brain (lane B) were separated by TLC and visualized with orcinol reagent. Glycolipids cross-reacting with the epitope of Gb3 were identified by immunostaining on TLC-blotted PVDF membranes (lane C from the blot in lane A; lane D from the blot in lane B) with an anti-P^k MAb, followed by treatment with peroxidase-conjugated goat anti-mouse IgM F(ab')₂ and DAB-H₂O₂. The TLC-blotted membranes used for lane D was incubated with 1 μg of Stx2 per ml; and glycolipids to which Stx2 bound were visualized by immunostaining with an anti-Stx2 MAb, followed by treatment with biotinylated anti-mouse IgG F(ab')₂, avidin-peroxidase complex, and DAB-H₂O₂ (lane E).

staining with an anti-Stx2 MAb (lane E) at the position corresponding to Gb3 on the TLC-blotted membrane as seen in lanes C and D.

Apoptosis in the brain after infection. Frozen sections of brain tissues from six PCM mice infected with Sm^rN-9 were prepared for in situ TUNEL experiments at 10 days postinfection. Widespread apoptosis was observed in brain tissues in five out of six infected PCM mice, one of which is presented in Fig. 3. The mice whose brain tissues had many TUNEL-positive cells exhibited neurologic symptoms after day 5 of infection, and all were in a moribund state on day 10 postinfection. Approximately 28% of brain cells (56 ± 12/200 cells) in the sections from individual mice were TUNEL positive; such apoptotic cells were detected in the cerebellum, hippocampus, and brain stem samples from mice infected with Sm^rN-9. In contrast, only a background level of apoptosis (4 ± 2/200 cells; about 2%) was found in these areas of PCM mice inoculated with 2 × 10⁶ CFU of E. coli NP-4 and in those of well-nourished mice infected with the same dose of Sm^rN-9.

Cytotoxicity to HUVEC of Stx and cytokines. To explore the cooperation between Stx and inflammatory cytokines in causing cell damage to HUVEC, the effect of cytokines on the intracellular processing of fluorescein-labeled Stx2 was examined. HUVEC were incubated with the fluorescein-labeled toxin (100 ng/ml) in the presence or absence of TNF-α (20 U/ml), IL-1β (15 U/ml), or IL-6 (35 U/ml). As shown in Fig. 4, only TNF-α at 20 U/ml decreased the intensity of fluorescence per cell during 24 h of incubation. But none of these cytokines altered the binding of Stx2 to the surface of HUVEC during the first 12 h of incubation, since the mean fluorescence intensity per cell at 12 h of incubation remained at the same level, irrespective of the cytokines used. Microscopic observation, however, showed that the fluorescence intensity varied with

individual cells in each culture group during the first 12 h of incubation, suggesting heterogeneity of cultured HUVEC with respect to Stx binding (Fig. 5A). Interestingly, the decrease in the fluorescence intensity of HUVEC cultured with Stx2 and TNF-α was associated with intracellular compartmentalization of the labeled toxin during the next 12 h of incubation (Fig. 5B). In contrast, neither IL-1β nor IL-6 microscopically enhanced the intracellular compartmentalization of Stx2 in HUVEC (data not shown).

To determine the relationship between the enhanced intracellular compartmentalization of Stx2 and cell damage, TUNEL and LDH release assays were performed. A 48 h-incubation of HUVEC with 100 ng of Stx2 per ml induced 12% ± 5% TUNEL-positive cells, and incubation with TNF-α (20 U/ml) induced only 7% ± 3% positive cells (Fig. 6). However, simultaneous addition of Stx2 (100 ng/ml) and TNF-α (20 U/ml) to cultures of HUVEC resulted in about 47% ± 6% of the cells becoming TUNEL positive. Agarose gel electrophoresis demonstrated the nucleosomal ladder pattern of DNA extracted from HUVEC incubated with Stx2 and TNF-α for 48 h (Fig. 7), indicating that these TUNEL-positive cells underwent apoptosis. DNA preparations extracted from HUVEC treated with Stx2 alone or TNF-α alone presented less or no DNA fragmentation. Cytotoxicity as determined by the LDH release assay at 72 h of incubation was significantly increased (P <
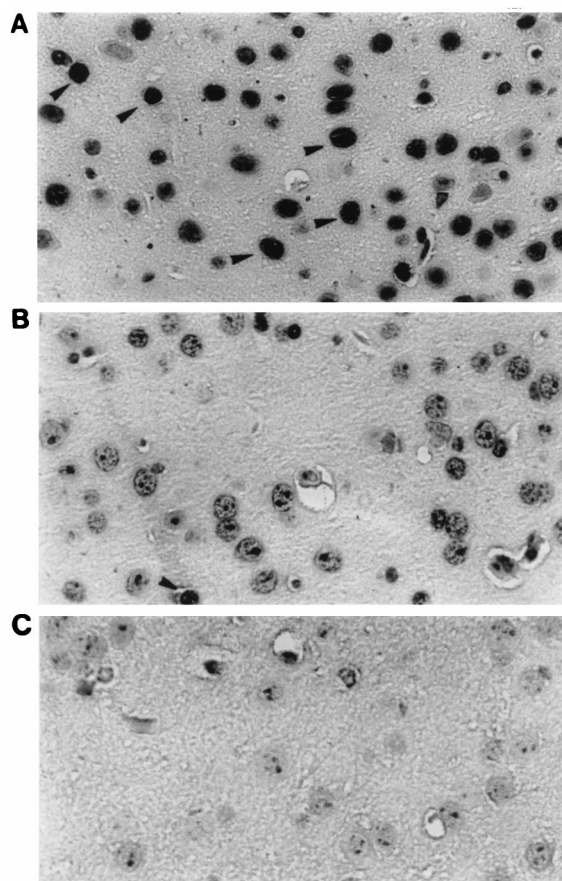

FIG. 3. Apoptotic cells demonstrated by the TUNEL assay in sections of the hippocampus area prepared from PCM mice at 10 days postinfection. (A) PCM mouse infected with E. coli Sm^rN-9, developing neurologic symptoms from day 5 of infection; (B) PCM mouse infected with E. coli NP-4, presenting no abnormal symptoms; (C) negative control for panel A (nick end labeling done in the absence of TdT). Arrow heads, TdT-positive cells; original magnification, ×350.
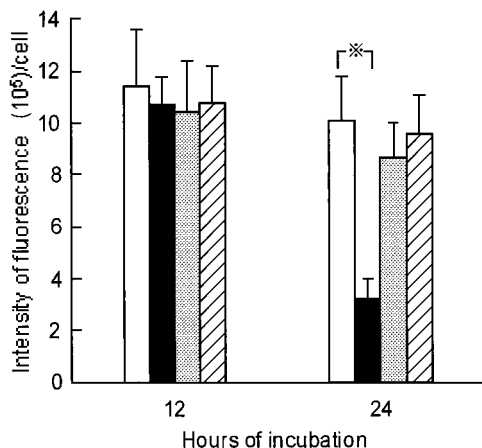
FIG. 4. Fluorescence intensity of HUVEC during incubation with fluorescent dye-labeled Stx2 in the presence or absence of TNF-α. HUVEC (5×10^4) were incubated with Oregon Green 488-labeled Stx2 (100 ng/ml) alone (□) or in the presence of TNF-α (20 U/ml) (■), IL-1β, (15 U/ml) (▦), or IL-6 (35 U/ml) (▨). At 12 and 24 h of incubation, the cells were washed three times with PBS, 50 cells were randomly selected, and the fluorescence intensity of each cell was quantified with a computer-assisted fluorescence scanning confocal microscope. Data were obtained from three independent experiments, each performed in triplicate. Results are expressed as the mean ± SD for nine determinants. Each bar represents SD. ※, $P < 0.01$.

0.01) in the presence of Stx2 and TNF-α: from 14.3% (Stx2 alone) or <5.0% (TNF-α alone) to 63.5% (Stx2 plus TNF-α) (Table 1). In contrast, neither IL-1β (15 U/ml) nor IL-6 (35 U/ml) displayed the synergistic effect when added to HUVEC monolayers at the initiation of incubation with Stx2 (data not shown). An anti-TNF-α MAb (50 ng/ml) significantly reduced both apoptosis ($P < 0.05$) (Fig. 6) and cytotoxicity ($P < 0.01$) (Table 1) caused by the synergistic effect of Stx2 and TNF-α.
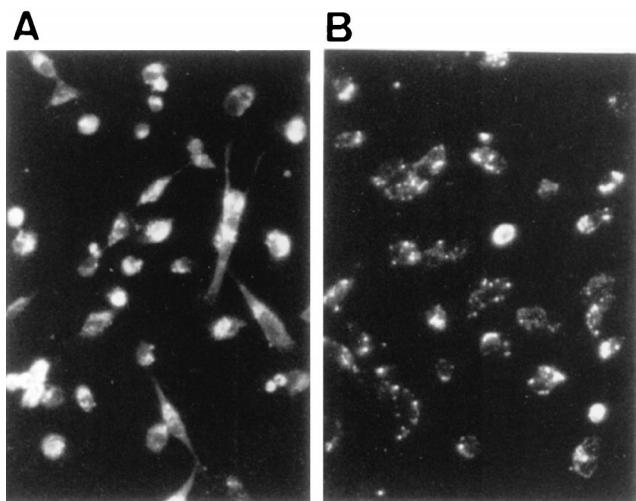

FIG. 5. Acceleration of the intracellular compartmentalization of fluorescent dye-labeled Stx2 in HUVEC by TNF-α. HUVEC (5×10^4) were incubated with fluorescent dye-labeled Stx2 (100 ng/ml) in the presence or absence of TNF-α (20 U/ml). (A) Incubation of HUVEC with Stx2 for 12 h, showing the cells densely stained with fluorescence. There was no apparent difference in the microscopic characteristics of the labeled toxin bound to HUVEC between the presence and the absence of TNF-α, IL-1β, or IL-6 during the first 12 h of incubation. (B) Incubation of HUVEC with Stx2 and TNF-α for a further 12 h, showing the decrease in fluorescence intensity of individual cells due to the intracellular compartmentalization of the toxin. Microscopic characteristics of the labeled toxin after 24-h incubation of HUVEC with IL-1β or IL-6 remained similar to those observed at 12 h. Original magnification, ×200.
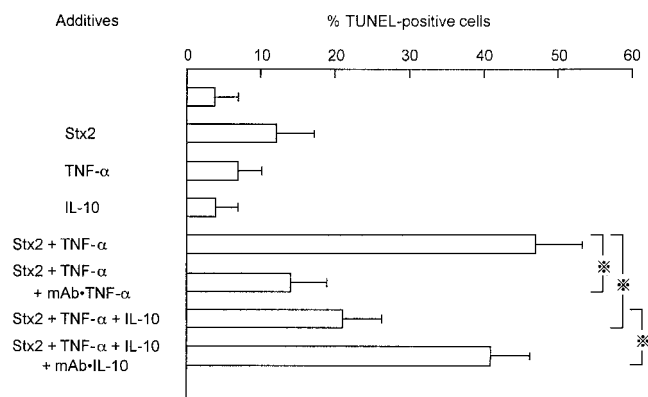

FIG. 6. Effect of cytokines on the induction of apoptosis in HUVEC by Stx2. HUVEC monolayers were incubated with Stx2 (100 ng/ml) alone, TNF-α (20 U/ml) alone, or IL-10 (20 U/ml) alone or with Stx2 and TNF-α. Levels of apoptosis were determined by the TUNEL assay at 48 h of incubation. An anti-TNF-α MAb was used at 50 ng/ml, and an anti-IL-10 MAb was used at 3 μg/ml. ※, $P < 0.05$.

Twenty units of IL-10 also reduced both apoptosis ($P < 0.05$) (Fig. 6) and cytotoxicity ($P < 0.01$) (Table 1) induced by Stx2 and TNF-α, and its antiapoptotic activity was nearly comparable to that of anti-TNF-α MAb (50 ng/ml).

Relationship between Stx2 and TNF-α in induction of apoptosis in HUVEC. The relationship between Stx2 and TNF-α in induction of apoptosis in HUVEC was examined by systematically varying the order in which cells were exposed to each agent. HUVEC first exposed to Stx2, TNF-α, or medium (for 6 h) and subsequently cultured with medium (for 42 h) manifested baseline levels of apoptosis only after 48 h of incubation (3.0 to 3.5%) (Table 2). Cultures first exposed to TNF-α and then to Stx2 demonstrated apoptosis in about 43.8% of HUVEC, the level of which was nearly comparable to the magnitude of apoptosis in response to 48-h incubation after simultaneous addition of Stx2 and TNF-α (44.9% ± 6.5%). In contrast, HUVEC first exposed to Stx2 manifested a significantly reduced apoptotic response to subsequent exposure to TNF-α (9.8% ± 3.3%) ($P < 0.01$ compared to positive controls), the level of which was similar to that obtained with subsequent exposure to Stx2 (11.4% ± 3.9%). In addition, initial
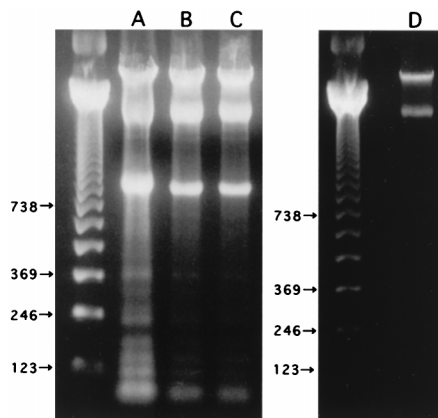

FIG. 7. Agarose gel electrophoresis of DNA from HUVEC. HUVEC were incubated with Stx2 (100 ng/ml) and TNF-α (20 U/ml) (A), Stx2 alone (B), TNF-α alone (C), or medium alone (D). DNA was extracted after a 48-h incubation and fractionated on a 2% agarose gel. The positions of 123-, 246-, 369-, and 738-bp bands of the 123-bp DNA molecular weight marker are shown.

TABLE 1. Effects of cytokines on Stx cytotoxicity to HUVEC[a]

HUVEC cultured with:	Cytotoxicity (%)
Medium only	<5
TNF-α (20 U/ml)	<5
IL-1β (15 U/ml)	<5
IL-6 (35 U/ml)	<5
IL-10 (20 U/ml)	<5
Stx2 (100 ng/ml)	
Alone	14.3 ± 3.6
+TNF-α	63.5 ± 4.1[b]
+IL-1β	19.5 ± 3.8[c]
+IL-6	15.7 ± 4.4[c]
+IL-10	<5
Stx2 + TNF-α	
+MAb to TNF-α (50 ng/ml)	18.8 ± 3.6[d]
+IL-10 (20 U/ml)	20.7 ± 4.2[d]

[a] HUVEC were cultured with various stimulants. After 72 h of culture, cytotoxicity was determined by the LDH release assay. Data were obtained from three different experiments, each including five determinants for cytotoxicity. Results are expressed as the mean ± SD for 15 determinants.
[b] $P < 0.01$ compared to Stx2 alone.
[c] Not significant compared to Stx2 alone.
[d] $P < 0.01$ compared to Stx2 plus TNF-α.

exposure to Stx2 significantly ($P < 0.01$) suppressed the apoptotic response to subsequent exposure to Stx2 and TNF-α (14.9% ± 4.8%) compared to cultures exposed first to medium and then to Stx2 and TNF-α (42.8% ± 6.7%, positive controls). In contrast, initial exposure to TNF-α did not affect the apoptotic response of HUVEC subsequently incubated with Stx2 and TNF-α (46.7% ± 5.9%).

DISCUSSION

Several investigators have shown that inflammatory cytokines, particularly TNF-α and IL-1β, are capable of enhancing Stx toxicity to vascular endothelial cells expressing Gb3 (14, 18, 31, 34). Isogai et al. (11) have reported that TNF-α in the tissue but not in the serum may contribute to the pathogenesis of brain damage caused by Stx. We attempted to identify Stx receptors in the mouse brain and also to examine how HUVEC are injured by the synergistic effect of inflammatory cytokines and Stx.

Although Stx has not been detected in sera of HUS patients, the toxin was measurable by EIA in the sera of PCM mice from days 3 through 5 after infection. Because of its molecular size, Stx must first damage the BBB in order to reach the CNS. This would possibly occur in the presence of TNF-α and/or IL-1β (18). In this study, serum levels of TNF-α were increased in infected PCM mice before Stx was detected in the serum. Our preliminary study has shown that PCM mice manifest higher levels of TNF-α response after an injection of bacterial endotoxin than do well-nourished animals. Such an immunological disposition in PCM mice seems to account for the early production of TNF-α in the blood after infection.

Stx2 did not equally bind to cultured HUVEC in this study; the intensity of fluorescence microscopically varied with individual cells during 12 h of incubation. Obrig et al. (22) have reported that basal levels of Gb3 are approximately 50 times higher in human renal endothelial cells than in HUVEC. Moreover, HUVEC obtained from individual umbilical cords

differ in their sensitivities to Shiga toxin (22). Thus, the expression levels of Gb3 may differ among individual cultured HUVEC. Nevertheless, TNF-α rapidly decreased the fluorescence intensity of the cells. Stx bound to Gb3 has been shown to be taken up intracellularly through coated vesicles and transported in a retrograde manner to the endoplasmic reticulum via the *trans*-Golgi network (28), and Stx is processed by a trypsin-like cleavage to generate A1 and A2 subunits for full expression of its cytotoxicity (5). Thus, both the decrease in fluorescence intensity and the increased intracellular compartmentalization of labeled Stx2 may result from the acceleration of intracellular processing of Stx2 by TNF-α. Since the degree of cytotoxicity at 72 h almost paralleled that of apoptosis as determined by TUNEL assay at 48 h, death of HUVEC caused by Stx2 and TNF-α is likely to result mainly from apoptosis. This assumption is supported by the nucleosomal ladder pattern of DNA extracted from HUVEC stimulated with Stx2 and TNF-α for 48 h. IL-1β is also a potent stimulant for HUVEC to induce Gb3 expression (14, 18), but such an effect is not apparent unless the cells are preincubated with IL-1β at least for 24 h before exposure to the toxin (14).

In contrast, IL-10 reduced apoptosis in HUVEC cultured with Stx2 and TNF-α. The reason why the present study dealt with IL-10 is that serum levels of IL-10 were elevated to a significant extent in HUS patients (21). In fact, IL-10 levels were elevated in sera of infected PCM mice. However, IL-10 has a variety of biological activities, and its role in infection with E. coli O157:H7 remains to be determined.

Recently, endothelial cell apoptosis by TNF-α was shown to be enhanced by inhibitors of protein synthesis (25, 38). Normally, TNF-α does not injure human endothelial cells, but it can cause apoptosis of the cells cocultured with either the protein synthesis inhibitor cycloheximide or the lipid mediator ceramide (24). Moreover, TNF receptors are required for TNF-induced apoptosis in microvascular endothelial cells (19). Taking these findings together, we hypothesized that Stx can potentiate TNF-α-induced apoptosis in HUVEC, rather than TNF-α enhancing Stx cytotoxicity, since HUVEC are at least 10^6-fold less susceptible to Stx than Vero cells (31). In this study, short-term exposure of HUVEC to Stx significantly suppressed the apoptotic response to subsequent culture with TNF-α. In contrast, initial exposure to TNF-α induced apoptosis in HUVEC during subsequent incubation with Stx, the level of which was comparable to that induced by 48-h continuous culture with these two agents. These results were consis-

TABLE 2. Relationship between Stx2 and TNF-α in induction of apoptosis in HUVEC[a]

Initial exposure (6 h)	% Apoptotic cells after secondary exposure (42 h) to:			
	Medium	TNF-α	Stx2	Stx2 + TNF-α
Medium only	3.0 ± 1.4	5.2 ± 2.7	9.8 ± 5.6	42.8 ± 6.7[e]
Stx2 (100 ng/ml)	3.5 ± 1.6	9.8 ± 3.3[b]	11.4 ± 3.9[d]	14.9 ± 4.8[f]
TNF-α (20 U/ml)	3.1 ± 0.8	6.6 ± 3.7[c]	43.8 ± 7.5[e]	46.7 ± 5.9[e]

[a] Simultaneous addition of Stx2 and TNF-α as a positive control resulted in 44.9 ± 6.4% of HUVEC becoming TUNEL positive after 48 h of incubation.
[b] Not significant compared to HUVEC first exposed to Stx2 and subsequently cultured in Stx2.
[c] $P < 0.01$ compared to HUVEC first exposed to TNF-α and subsequently cultured in Stx2.
[d] $P < 0.01$ compared to HUVEC first exposed to TNF-α and subsequently cultured in Stx2.
[e] Not significant compared to positive controls.
[f] $P < 0.01$ compared to HUVEC first exposed to medium and subsequently cultured in Stx2 and TNF-α.

tent with the report by Polunovsky et al. (25) showing the synergistic effect of TNF-α and cycloheximide on endothelial cells. Commitment to apoptosis in HUVEC by TNF-α therefore may be manifest only after subsequent inhibition of protein synthesis by Stx2. In addition, the present study has proved the hypothesis (18) that TNF treatment of HUVEC influences the uptake or activation of Stx. In fact, injury of HUVEC was completely blocked by an anti-TNF-α MAb. Moreover, the present findings are in agreement with the report (11) showing that a TNF-α inhibitor (protease inhibitor) reduced the pathological symptoms in mice after infection with Stx-producing *E. coli* O157:H7.

Neutral glycolipid fraction of mouse brains contained Gb3 which was functionally active. Moreover, frozen sections of the brain from infected PCM mice contained higher numbers of TUNEL-positive cells compared to those from control PCM mice infected with a nonpathogenic *E. coli* strain. Although a TNF-α response in the blood was detected on day 2 of infection, circulating TNF-α normally does not enter the CNS unless the BBB is injured. Nevertheless, this cytokine was detected in brain tissues of infected PCM mice as early as 3 days after infection. At present, it is most probable that TNF-α enters the CNS through the BBB damaged by circulating TNF-α and Stx.

In conclusion, the rapid production of TNF-α after infection is crucial to the injury of vascular endothelial cells; TNF-α promotes the rapid intracellular activation of Stx, and in turn, activated Stx potentiates TNF-α-induced apoptosis in the cells. In this synergistic action, the cells should be first exposed to TNF-α. Such cell damage must be a prerequisite to the initiation of brain damage after infection with Stx-producing *E. coli*.

REFERENCES

1. Brodin, N. T., J. Dahmén, B. Nilsson, L. Messeter, S. Martensson, J. Heldrup, H. O. Sjögren, and A. Lundblad. 1988. Monoclonal antibodies produced by immunization with neoglycoproteins containing Galα1-4Galβ1-4Glc-O and Galα1-4Galβ1-4GlcNAc-O residues: useful immunochemical and cytochemical reagents for blood group P antigens and a differentiation marker in Burkitt lymphoma and other B-cell malignancies. Int. J. Cancer **42:**185–194.
2. Fujii, J., T. Kita, S. Yoshida, T. Takeda, H. Kobayashi, N. Nakata, K. Ohsato, and Y. Mizuguchi. 1994. Direct evidence of neuron impairment by oral infection with verotoxin-producing *Escherichia coli* O157:H- in mitomycin-treated mice. Infect. Immun. **62:**3447–3453.
3. Fujii, J., Y. Kinoshita, T. Kita, A. Higure, T. Takeda, N. Tanaka, and S. Yoshida. 1996. Magnetic resonance imaging and histopathological study of brain lesions in rabbits given intravenous verotoxin 2. Infect. Immun. **64:**5053–5060.
4. Fujii, J., Y. Kinoshita, Y. Yamada, T. Yutsudo, T. Kita, T. Takeda, and S. Yoshida. 1998. Neurotoxicity of intrathecal Shiga toxin 2 and protection by intrathecal injection of anti-Shiga toxin 2 antiserum in rabbits. Microb. Pathog. **25:**139–146.
5. Garred, Ø., E. Dubinina, P. K. Holm, S. Olsnes, B. Deurs, J. V. Kozlov, and K. Sandvig. 1995. Role of processing and intracellular transport for optimal toxicity of Shiga toxin and toxin mutants. Exp. Cell Res. **218:**39–49.
6. Gavrieli, Y., Y. Sherman, and S. A. Ben-Sasson. 1992. Identification of programmed cell death in situ via specific labeling of nuclear DNA fragmentation. J. Cell Biol. **119:**493–501.
7. Glaser, B. A., P. A. D'Amore, R. G. Michels, A. Patz, and A. Fenslau. 1980. Demonstration of vasoproliferative activity from mammalian retina. J. Cell Biol. **84:**298–304.
8. Hamano, S., Y. Nakanishi, T. Nara, T. Seki, T. Ohtani, T. Oishi, K. Joh, T. Oikawa, Y. Muramatsu, Y. Ogawa, and S. Akashi. 1993. Neurological manifestations of hemorrhagic colitis in the outbreak of *Escherichia coli* O157:H7

infection in Japan. Acta Pediatr. **82:**454–458.
9. Harel, Y., M. Silva, B. Giroir, A. Weinberg, T. B. Cleary, and B. Beutler. 1993. A reporter transgene indicates renal-specific induction of tumor necrosis factor (TNF) by Shiga-like toxin. J. Clin. Investig. **92:**2110–2116.
10. Hogan, M. M., P. Y. Perera, and S. N. Vogel. 1989. Examination of macrophage cell surface antigen regulation by rIFN-γ and IFN-α/β utilizing digital imaging by a novel laser detection system. Anchored cell analysis station (ACAS) 470. J. Immunol. Methods **123:**9–18.
11. Isogai, E., H. Isogai, K. Kimura, T. Hayashi, T. Kubota, N. Fujii, and K. Takeshi. 1998. Role of tumor necrosis factor alpha in gnotobiotic mice infected with an *Escherichia coli* O157:H7 strain. Infect. Immun. **66:**197–202.
12. Karmali, M. A. 1989. Infection by verocytotoxin-producing *Escherichia coli*. Clin. Microbiol. Rev. **2:**15–38.
13. Karpman, D., H. Connell, M. Svensson, F. Scheutz, P. Alm, and C. Svanborg. 1997. The role of lipopolysaccharide and Shiga-like toxin in a mouse model of *Escherichia coli* O157:H7 infection. J. Infect. Dis. **175:**611–620.
14. Kaye, S. A., C. B. Louise, B. Boyd, C. A. Lingwood, and T. G. Obrig. 1993. Shiga toxin-associated hemolytic uremic syndrome: interleukin-1β enhancement of Shiga toxin cytotoxicity toward human vascular endothelial cells in vitro. Infect. Immun. **61:**3886–3891.
15. Kundu, S. K. 1981. DEAE-silica gel and DEAE-controlled porous glass as ion exchangers for the isolation of glycolipids. Methods Enzymol. **72:**174–185.
16. Kurioka, T., Y. Yunou, and E. Kita. 1998. Enhancement of susceptibility to Shiga toxin-producing *Escherichia coli* O157:H7 by protein calorie malnutrition in mice. Infect. Immun. **66:**1726–1734.
17. Ladisch, S., and B. Gillard. 1985. A solvent partition method for microscale ganglioside purification. Anal. Biochem. **146:**220–231.
18. Louise, C. B., and T. G. Obrig. 1991. Shiga toxin-associated hemolytic-uremic syndrome: combined cytotoxic effects of Shiga toxin, interleukin-1β, and tumor necrosis factor alpha on human vascular endothelial cells in vitro. Infect. Immun. **59:**4173–4179.
19. Lucas, R., I. Garcia, Y. R. A. Donati, M. Hribar, S. J. Mandriota, C. Giroud, W. A. Buurman, L. Fransen, P. M. Suter, G. Nuñez, M. S. Pepper, and G. E. Grau. 1998. Both TNF receptors are required for direct TNF-mediated cytotoxicity in microvascular endothelial cell. Eur. J. Immunol. **28:**3577–3586.
20. Mangeney, M., C. A. Lingwood, S. Taga, B. Caillou, T. Tursz, and J. Wiels. 1993. Apoptosis induced in Burkitt's lymphoma cells via Gb3/CD77, a glycolipid antigen. Cancer Res. **53:**5314–5319.
21. Murata, A., T. Shimazu, T. Yamamoto, N. Taenaka, K. Nagayama, T. Honda, H. Sugimoto, M. Monden, N. Matsuura, and S. Okada. 1998. Profiles of circulating inflammatory- and anti-inflammatory cytokines in patients with hemolytic uremic syndrome due to *E. coli* O157 infection. Cytokine **10:**544–548.
22. Obrig, T. G., C. B. Louise, C. A. Lingwood, B. Boyd, L. Barley-Maloney, and T. O. Daniel. 1993. Endothelial heterogeneity in Shiga toxin receptors and responses. J. Biol. Chem. **268:**15484–15488.
23. Pai, C. H., J. K. Kelly, and G. L. Meyers. 1986. Experimental infection of infant rabbits with verotoxin-producing *Escherichia coli*. Infect. Immun. **51:**16–23.
24. Pober, J. S. 1998. Activation and injury of endothelial cells by cytokines. Pathol. Biol. **46:**159–163.
25. Polunovsky, V. A., C. H. Wendt, D. H. Ingbar, and M. S. Peterson. 1994. Induction of endothelial cell apoptosis by TNF-α: modulation by inhibitors of protein synthesis. Exp. Cell Res. **214:**584–594.
26. Richardson, S. E., T. A. Rotman, V. Jay, C. R. Smith, L. F. Becke, M. Petric, N. F. Olivieri, and M. A. Karmali. 1992. Experimental verocytotoxemia in rabbits. Infect. Immun. **60:**4154–4167.
27. Saito, T., and S. Hakomori. 1971. Quantitative isolation of total glycosphingolipids from animal cells. J. Lipid Res. **12:**257–259.
28. Sandvig, K., Ø. Garred, K. Prydz, J. V. Kozlov, S. H. Hansen, and B. van Deurs. 1992. Retrograde transport of endocytosed Shiga toxin to the endoplasmic reticulum. Nature **358:**510–512.
29. Sharefkin, J. B., K. D. Fairchild, R. A. Albus, D. F. Cruess, and N. M. Rich. 1986. The cytotoxic effect of surgical glove powder particles on adult human vascular endothelial cell cultures: implications for clinical uses of tissues culture techniques. J. Surg. Res. **41:**463–472.
30. Taga, S., K. Carlier, Z. Mishal, C. Capoulade, and M. Mangeney. 1997. Intracellular signaling events in CD77-mediated apoptosis of Burkitt's lymphoma cells. Blood **90:**2757–2767.
31. Tesh, V. L., J. E. Samuel, L. P. Perera, J. B. Sharefkin, and A. D. O'Brien. 1991. Evaluation of the role of Shiga and Shiga-like toxins in mediating direct damage to human vascular endothelial cells. J. Infect. Dis. **164:**344–352.
32. Tzipori, S., C. W. Chow, and H. R. Powell. 1988. Cerebral infection with *Escherichia coli* O157:H7 in humans and gnotobiotic piglets. J. Clin. Pathol. **41:**1099–1103.
33. Tzipori, S., K. I. Wachsmuth, C. Chapman, R. Birner, J. Brittingham, C. Jackson, and J. Hogg. 1986. Studies on the pathogenesis of hemorrhagic colitis caused by *Escherichia coli* O157:H7 in gnotobiotic piglets. J. Infect. Dis. **154:**712–716.

34. **Van De Kar, N. C. A. J., T. Kooistra, M. Vermeer, W. Lesslauer, L. A. H. Monnens, and V. W. M. van Hinsbergh.** 1995. Tumor necrosis factor-alpha induces endothelial galactosyl transferase activity and verocytotoxin receptors. Role of specific tumor necrosis factor receptors and protein kinase C. Blood **85:**734–743.

35. **Wadolkowski, E. A., J. A. Burris, and A. D. O'Brien.** 1990. Mouse model for colonization and disease caused by enterohemorrhagic *Escherichia coli* O157:H7. Infect. Immun. **58:**2438–2445.

36. **Wadolkowski, E. A., L. M. Sung, J. A. Burris, J. E. Samuel, and A. D. O'Brien.** 1990. Acute renal tubular necrosis and death of mice orally infected with *Escherichia coli* strains that produce Shiga-like toxin type II. Infect. Immun. **58:**3959–3965.

37. **Weinberg, D. S., K. A. Ault, M. Gurley, and G. S. Pinkus.** 1986. The human lymph node germinal center cell: characterization and isolation by using two-color flow cytometry. J. Immunol. **137:**1486–1494.

38. **Woods, K. M., and S. K. Chapes.** 1993. Three distinct cell phenotype of induced TNF cytotoxicity and their relationship to apoptosis. J. Leukoc. Biol. **53:**37–44.

39. **Yutsudo, T., N. Nakabayashi, T. Hirayama, and Y. Takeda.** 1987. Purification and some properties of a Vero toxin from *Escherichia coli* O157:H7 that is immunologically unrelated to Shiga toxin. Microb. Pathog. **3:**21–30.